



Collective nonlinear optical effects in plasmonic nanohole ensembles of different rotational symmetries

Citation

Bautista, G., Dreser, C., Zang, X., Kern, D., Kauranen, M., & Fleischer, M. (2018). Collective nonlinear optical effects in plasmonic nanohole ensembles of different rotational symmetries. In *CLEO: QELS_Fundamental Science 2018* [FW3G.3] The Optical Society; OSA. https://doi.org/10.1364/CLEO_QELS.2018.FW3G.3

Year

2018

Version

Peer reviewed version (post-print)

Link to publication

[TUTCRIS Portal \(http://www.tut.fi/tutcris\)](http://www.tut.fi/tutcris)

Published in

CLEO

DOI

[10.1364/CLEO_QELS.2018.FW3G.3](https://doi.org/10.1364/CLEO_QELS.2018.FW3G.3)

Copyright

© 2018 Optical Society of America. One print or electronic copy may be made for personal use only. Systematic reproduction and distribution, duplication of any material in this paper for a fee or for commercial purposes, or modifications of the content of this paper are prohibited.

License

Unspecified

Take down policy

If you believe that this document breaches copyright, please contact cris.tau@tuni.fi, and we will remove access to the work immediately and investigate your claim.

Collective nonlinear optical effects in plasmonic nanohole ensembles of different rotational symmetries

Godofredo Bautista,^{1,*} Christoph Dreser,^{2,3} Xiaorun Zang,¹ Dieter P. Kern,^{2,3} Martti Kauranen¹ and Monika Fleischer^{2,3}

¹Laboratory of Photonics, Tampere University of Technology, Korkeakoulunkatu 3, 33720 Tampere, Finland

²Institute for Applied Physics, University of Tübingen, Auf der Morgenstelle 10, 72076 Tübingen, Germany

³Center for Light-Matter-Interaction, Sensors and Analytics LISA⁺, University of Tübingen, Auf der Morgenstelle 15, 72076 Tübingen, Germany
*godofredo.bautista@tut.fi

Abstract: We use cylindrical vector beams to investigate second-harmonic generation from rotationally symmetric arrangements of plasmonic nanoholes. The second-harmonic efficiency is shown to depend strongly on collective interactions between the nanoholes.

OCIS codes: (180.4315) Nonlinear microscopy; (250.5403) Plasmonics; (190.2620) Harmonic generation and mixing; (260.5430) Polarizations

1. Introduction

There is an ongoing interest in tailoring nonlinear optical effects, such as second-harmonic generation (SHG), using single metal nanostructures and their ensembles [1]. Alternatively, complementary nanostructures, i.e., nanoholes in thin metal films, have been used to modify SHG at the nanoscale [2]. In addition, the SHG efficiency from nanoholes was found to be strongly dependent on their geometry [3,4] and arrangement [4]. Most importantly, collective effects between adjacent nanoholes and their interactions with the surface plasmon of the metal film are expected to provide new ways to modify SHG [5]. To date, collective SHG effects in coupled nanoholes remain unexplored. In this paper, we demonstrate tailoring of SHG in rotationally symmetric arrangements of nanoholes using *cylindrical vector beams* (CVB) with radial and azimuthal polarizations. The SHG efficiency is shown to depend strongly on collective interactions between the coupled nanoholes.

2. Samples

Multiple configurations of rectangular nanoholes were studied. To realize structures of different rotational symmetries, the number of nanoholes in each configuration was varied from 2 to 16 (Fig. 1a). The spatial distribution of the nanoholes was carefully designed such that the long axis of the constituent nanoholes follows the transverse electric field distributions of radial (Fig. 1b) or azimuthal (Fig. 1c) CVBs in the focal plane. The nanoholes were milled in a 20-nm thin film of gold on a glass substrate. For each configuration, both the size of the nanoholes (length 160 nm and width 30 nm) and distance of the nanoholes from the center of the structure (460 nm) were kept fixed. These parameters are chosen in order to facilitate SHG microscopy of individual nanohole configurations. Shown in Figs. 1d,e are scanning electron microscopy (SEM) images of the real samples.

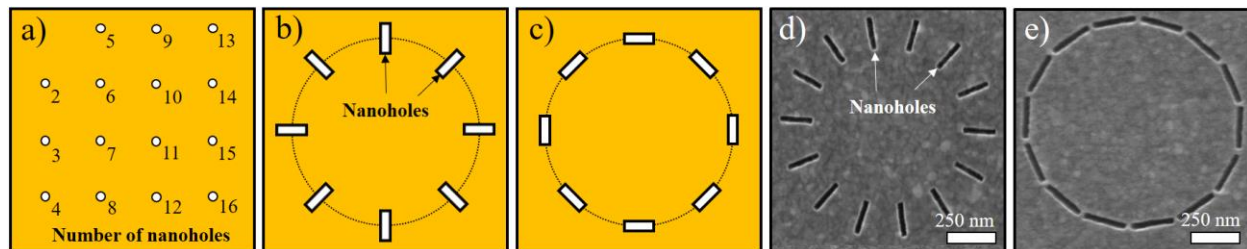


Fig. 1. a) Sample layout with varying number of nanoholes (from 2 to 16). b,c) Schematic diagrams of eight rectangular nanoholes (length 160 nm and width 30 nm) that are spatially arranged to follow the transverse electric focal fields of (b) radial and (c) azimuthal CVBs. The nanoholes are placed at a distance of 460 nm from the center of the overall structure. d,e) SEM images of the fabricated (d) radial and (e) azimuthal nanoholes.

3. SHG microscopy experiments and calculations

The samples were studied using a custom-built point-scanning nonlinear optical microscope [6]. A pulsed laser (pulse duration 140 fs, repetition rate 80 MHz, and wavelength 1060 nm) was used as the excitation source. After beam expansion and collimation, the beam was directed to a microscope objective (numerical aperture 0.8). The scattered SHG signals from the samples were collected in reflection, discriminated by appropriate optical filters and directed to a cooled photomultiplier tube. To generate CVBs, a mode-converter with a spatial filter was used.

To simulate SHG in the plasmonic nanoholes, we used the boundary element method (BEM) [6]. We considered nanoholes that are embedded in a thin extended disk of gold. The nanoholes have a thickness of t , width w , and length l . The nanoholes form a rotationally symmetric structure with radius r . The disk has a thickness of $3t$ and radius R . R was chosen large enough so that significant light reflection from the disk periphery does not appear. We considered non-zero nonlinear susceptibility $\chi_{nnn}^{(2)}$ only on the defining surface of the nanohole and neglected the surface nonlinearity on the external boundary of the thin gold disk. The far-field scanning images of each nanohole configuration were calculated at the SH frequency using parameters that closely resemble the experiments.

4. Results and discussion

Due to Babinet's principle, an individual rectangular nanohole is expected to be excited when the magnetic component of the optical field is aligned with the long axis of the hole [7]. In consequence, our samples are collectively excited when radial samples are symmetrically illuminated with azimuthal CVB and vice versa, which we refer to as polarization anti-matching configurations (Figs. 2b,d). This excitation selectivity is further confirmed by the disappearance of the SHG signal at the same location when the polarization-matching CVB is used (Figs. 2a,c). In addition, we found that the SHG signals from the azimuthal nanoholes are generally weaker than those from their radial counterparts. For radial nanoholes that are symmetrically illuminated by the azimuthal CVB, the SHG signals increase with the number of nanoholes (Fig. 2b). For azimuthal nanoholes that are symmetrically illuminated by the radial CVB, the SHG signals increase and then decrease with the number of nanoholes leading to the silencing of SHG from the whole structure (Fig. 2d). The striking differences in the SHG behavior in these nanohole configurations suggest that the collective interactions among the nanoholes strongly influence the SHG of the whole structure. These experimental results have been reproduced qualitatively well in our BEM calculations (Figs. 2e,f). Altogether, our work shows the prospect of tailoring SHG efficiency in nanoholes of well-defined structural symmetries using CVBs. These results are general and applicable in the tailoring of other nonlinear processes such as third-harmonic generation and nonlinear photoluminescence in nanohole arrangements.

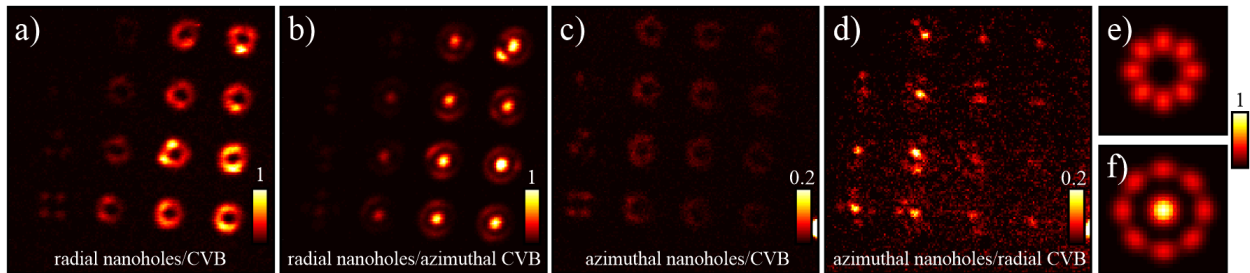


Fig. 2. a-d) Experimental far-field SHG scanning images of a,b) radial and c,d) azimuthal nanoholes that are excited by a,d) radial and b,c) azimuthal CVBs using the same experiment settings. The SHG images were acquired using an input power of 5 mW and a pixel dwell time of 50 ms. The layout is the same as in Fig. 1a. Image size: $18 \times 18 \mu\text{m}^2$. e,f) Calculated far-field SHG scanning images of eight azimuthally-configured nanoholes that are excited by e) azimuthal and f) radial CVBs. The parameters used in the calculations closely resemble the experiment. Image size: $5 \times 5 \mu\text{m}^2$.

5. References

- [1] M. Kauranen and A. V. Zayats, "Nonlinear plasmonics," *Nature Photon* **6**, 737–748 (2012).
- [2] J. A. van Nieuwstadt, M. Sandtke, R. H. Harmsen, F. B. Segerink, J. C. Prangsma, S. Enoch, and L. Kuipers, "Strong modification of the nonlinear optical response of metallic subwavelength hole arrays," *Phys Rev Lett.* **97**(14), 146102 (2006).
- [3] P. Schön, N. Bonod, E. Devaux, J. Wenger, H. Rigneault, T. W. Ebbesen, and S. Brasselet, "Enhanced second-harmonic generation from individual metallic nanoapertures," *Opt. Lett.* **35**, 4063–4065 (2010).
- [4] T. Xu, X. Jiao, G. P. Zhang, and S. Blair, "Second-harmonic emission from sub-wavelength apertures: Effects of aperture symmetry and lattice arrangement," *Opt. Express* **15**, 13894–13906 (2007).
- [5] A. Salomon, Y. Prior, M. Fedoruk, J. Feldmann, R. Kolkowski, and J. Zyss, "Plasmonic coupling between metallic nanocavities," *J. Opt.* **16**(11), 114012 (2014).
- [6] G. Bautista, M. J. Huttunen, J. Makitalo, J. M. Kontio, J. Simonen, and M. Kauranen, "Second-harmonic generation imaging of metal nano-objects with cylindrical vector beams," *Nano Lett* **12**, 3207–3212 (2012).
- [7] H. G. Booker, "Slot aerials and their relation to complementary wire aerials Babinet's principle," *IEEE J. Inst. Electr. Eng. Part III* **93**, 620–626 (1946).